

Development of an Automated Assistive Trainer Inspired by Neuro-developmental Treatment

Fu-Cheng Wang,^{1*} Yu-You Lin,¹ You-Chi Li,¹ Po-Yin Chen², and Chung-Huang Yu²

¹Department of Mechanical Engineering, National Taiwan University,
No. 1, Sec. 4, Roosevelt Road, Taipei 10617, Taiwan

²Department of Physical Therapy and Assistive Technology, National Yang-Ming University,
No. 155, Sec. 2, Linong Street, Taipei 11221, Taiwan

(Received November 14, 2019; accepted August 25, 2020)

Keywords: neuro-developmental treatment, gait training, rehabilitation, robust control, motion analysis

This paper introduces the development of an automated trainer that can conduct neuro-developmental treatment (NDT) rehabilitation for stroke patients. NDT training is a way to let patients have the feeling of walking with minimal intervention. During the training, therapists need to stabilize the patient's trunk and pelvis to stimulate the weight shift and pelvic rotation, and to assist limb control during the stance and swing phases to increase walking ability. Therefore, NDT rehabilitation is effective for stroke patients but labor-intensive for therapists. We have developed an automated NDT trainer that can mimic the therapists' intervention to reduce their workloads. First, we recruit subjects to conduct traditional NDT rehabilitation, where we apply a motion capture system to record the test subjects' motions and load cells to record the therapists' intervention force patterns during clinical NDT training. Second, we analyze the recorded data and develop an automated NDT trainer, which can detect the user's motions by the motion capture system and repeat the therapists' intervention by a closed-loop motor control system. Last, the designed trainer is applied to conduct NDT training for 10 stroke patients. The experimental results show that these test subjects' asymmetry of swing phases was improved after receiving the NDT training. In addition, the improvement by the trainer was greater than that by therapists, possibly because the trainer provides objective judgments and does not become fatigued. On the basis of the results, the developed trainer is deemed effective in providing suitable NDT training for stroke patients.

1. Introduction

Stroke is a common medical emergency with a high mortality rate. Those patients who survive cerebral vascular accidents usually require long-term treatment and lengthy rehabilitation.^(1,2) The expenditure for stroke treatments imposes a heavy load on society and on individuals; in the USA, each stroke patient spends about US\$18000 per year on rehabilitation treatments.⁽³⁾ In general, the purpose of rehabilitation is to recover the patients' capacity for independent living, particularly walking by themselves.

*Corresponding author: e-mail: fcw@ntu.edu.tw

<https://doi.org/10.18494/SAM.2020.2708>

Nomenclature			
F_{max}	Average maximum of the applied forces	C_{pre}	Phase lead pre-compensator
F_{min}	Average minimum of the applied forces	$Asym_{SP}$	Asymmetry of the swing phases
f	Dominant frequency	$SP_{paretic}$	Swing phase of the paretic limb
$G(s)$	Transfer function of the motor system	$SP_{non-paretic}$	Swing phase of the non-paretic limb
$C(s)$	Controller	A_{th}	Before treatment by therapists
u	Model input	B_{th}	In treatment by therapists
y	Model output	\bar{A}_{th}	After treatment by therapists
r	Force command	A_{mot}	Before treatment by motors
G_0	Nominal plant	B_{mot}	In treatment by motors
W	Weighting function	\bar{A}_{mot}	After treatment by motors
K_{∞}	Robust controller designed for G_0		

Several lower-limb rehabilitation robots have been developed to restore the mobility of affected limbs. These systems can be categorized according to their rehabilitation principles as follows:⁽⁴⁾

- (1) *Treadmill gait trainers*. For example, Colombo *et al.*⁽⁵⁾ designed a driven gait orthosis (DGO) to guide a patient's legs on a moving treadmill. They analyzed gait parameters and derived optimal training programs that can be reproduced by the DGO. Reinkensmeyer *et al.*⁽⁶⁾ developed a pneumatic gait-training robot that integrated a pelvic assist manipulator, gait orthosis, and body weight support (BWS) to assist leg and pelvic motions for patients with spinal cord injury.
- (2) *Foot-plate-based gait trainer*. For instance, Schmidt *et al.*⁽⁷⁾ proposed the HapticWalker, which consisted of programmable foot plates and a treadmill with force sensors, for wheelchair-mobilized patients. Wang *et al.*⁽⁸⁾ proposed an active gait trainer that can actively guide the ankle trajectories by a six-bar linkage and a motor.
- (3) *Overground gait trainer*. Patton *et al.*⁽⁹⁾ designed a robotic device, called KineAssist, for gait and balance training. The device provided partial BWS and postural control on the torso, so that therapists can manipulate the patient's legs during walking. Esquenazi *et al.*⁽¹⁰⁾ designed ReWalk, which is a powered exoskeleton allowing the user to walk independently without human assistance.
- (4) *Stationary gait and ankle trainer*. For example, Schmitt and Métrailler⁽¹¹⁾ presented MotionMaker, which had two orthoses with motors and sensors. The active device can manage real-time electrical stimulation to control leg movements according to the desired positions, speeds, and torques. Bradley *et al.*⁽¹²⁾ developed a rehabilitation system, called NeXOS, for the lower limbs of supine patients.
- (5) *Active foot orthoses*. For instance, Belforte *et al.*⁽¹³⁾ designed an active gait orthosis with electro-pneumatic circuits to assist locomotion for paraplegic subjects. Yu *et al.*⁽¹⁴⁾ proposed a compact compliant force control actuator for portable rehabilitation robots.

In contrast to the aforementioned devices that aimed to guide the patients to follow preset preferred gaits, neuro-developmental treatment (NDT) is a way to let the patients have the feeling of walking with minimal guidance and facilitation. During this training, the patients intentionally drive their center of gravity (COG) forward and balance themselves using striding

steps, so that they can feel the COG conversion between the feet.⁽¹⁵⁾ The key point of NDT intervention is to correct sensation and relearn the mechanism of normal patterns of postural and motor function in everyday life. Whereas other stroke gait training often provides only the actions by mechanical auxiliary equipment in clinics, NDT rehabilitation provides guided and induced interventions to achieve motor learning effects. Therefore, NDT training is effective for stroke survivors but is also very labor-intensive for therapists.^(15–17) For example, in a clinical NDT,^(18,19) one therapist stands behind the patient to adjust the pelvis motion and weight shifting, while a second therapist is positioned beside the paretic limb to assist stepping and limb control during the stance and swing phases. Hence, NDT rehabilitation can be very labor-intensive for therapists, meaning that patients usually receive insufficient training due to the shortage of therapist assistance.

In this paper, we propose a machine-aided NDT trainer that can relieve therapists' workloads by repeating the therapists' intervention to assist NDT rehabilitation for stroke patients. First, we recruit subjects to conduct traditional NDT rehabilitation. During the training, we apply a motion capture system (VZ 4000) to record the test subjects' motions and load cells (DPM-3) to record the therapists' intervention patterns. On the basis of these experimental data, we label the clinical key points and build an expert database to interpret the therapists' interventions. Second, we construct a motor mechanism based on the expert database to imitate the therapists' actions. Lastly, we integrate the system and recruit 10 stroke patients to conduct experiments. The experimental results show that the subjects' asymmetries of the swing phases were improved after using the automated NDT trainer. That is, the proposed trainer effectively improved the rehabilitation performance of the test subjects.

This paper is arranged as follows. Section 2 introduces the proposed automatic NDT trainer. We conducted clinical NDT training and recorded the therapists' interventions and the test subjects' motions during the training. On the basis of these data, we built an expert database to interpret the therapists' intervention. Then we designed a motor control system to imitate the therapists' actions. Section 3 presents the testing results of the automatic NDT trainer for the 10 stroke patients. We measured their gait data using the VZ 4000 motion capture system to evaluate the effectiveness of the trainer. Finally, we draw conclusions in Sect. 4.

2. Materials and Methods

The proposed automatic NDT trainer is shown in Fig. 1(a), where the test subject is connected to the BWS system, which provides the subject with support only when they were about to fall. Two ropes are attached near the subject's anterior-superior-iliac spine (ASIS) to stimulate the gaits. The subjects are guided by therapists and by the automatic device, which can repeat the therapists' actions. This method is different from conventional NDT rehabilitation, where the therapist directly applies forces on the patient's pelvis;^(18,19) however, the experimental results showed that the rope guidance achieves similar effects on the test subjects to the traditional hand-guiding method. The system structure is shown in Fig. 1(b). We applied a motion capture system (VZ 4000)⁽²⁰⁾ and two load cells (DPM-3)⁽²¹⁾ to record the test subjects' motions and the therapists' applied forces, respectively. The VZ 4000 can detect the LED markers attached

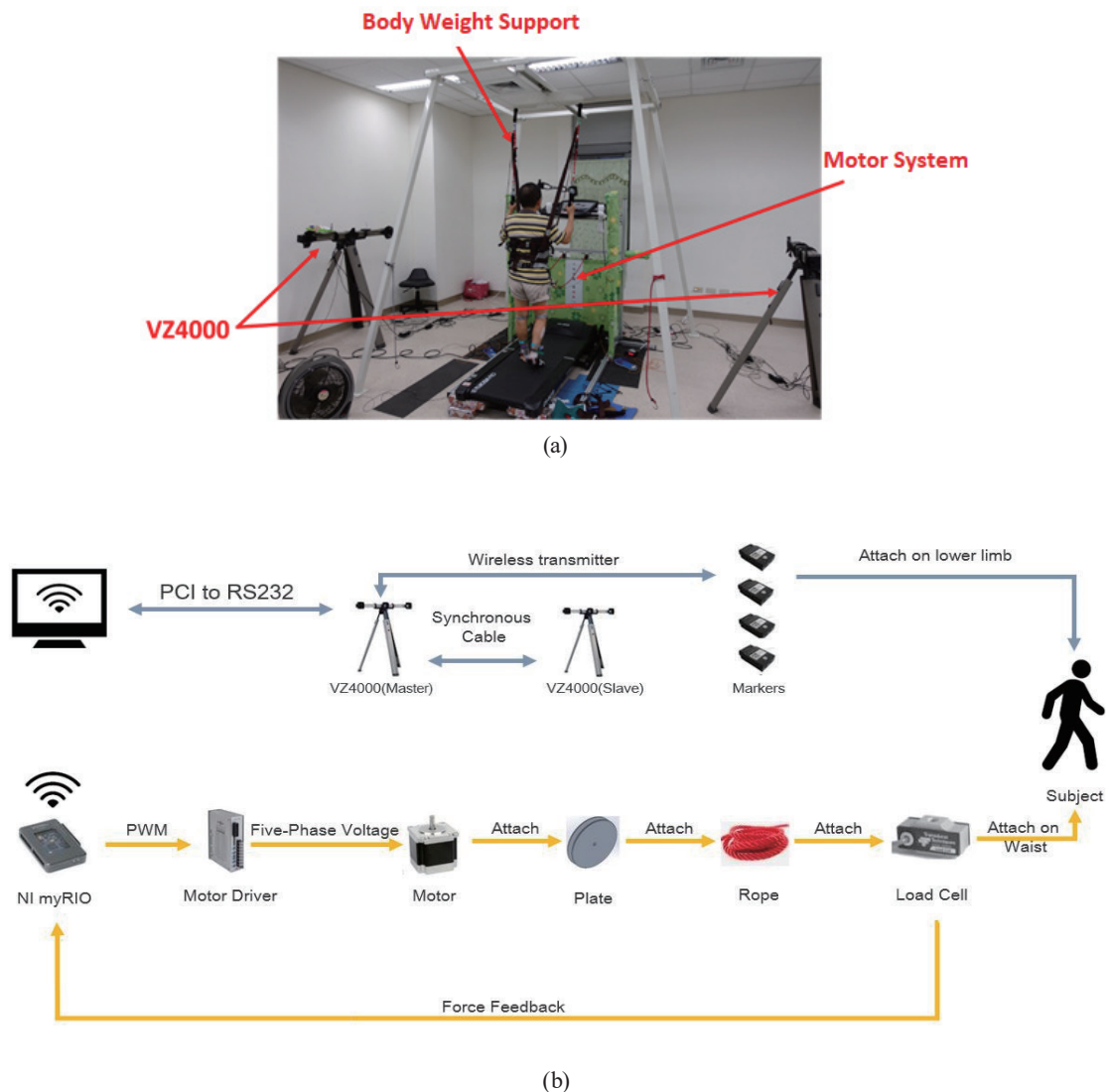


Fig. 1. (Color online) Proposed automatic NDT trainer. (a) Experimental layout. (b) System structure.

to the test subjects for gait measurements with a sampling rate of 100 Hz and a resolution of 0.015 mm at a distance of 1.2 m. We set the LED markers according to the Helen Hayes Marker Set:⁽²²⁾ four on the waist, two on the thighs, two on the knees, two on the shanks, two on the ankles, two on the toes, and two on the heels. The marker data were then transferred to obtain real-time position information. Because the therapists conducted NDT training by pulling the ropes to motivate the patient's gaits, we implemented load cells to detect the pulling forces. The measured position and force data were transmitted to an embedded National Instrument (NI) myRIO⁽²³⁾ microcontroller to identify the patterns of the therapists' actions. The data were then analyzed to build an expert database that described the therapists' intervention patterns. On the basis of the expert database, we constructed a motor control system to repeat the therapists' intervention patterns. The specifications of the system components are given in Table 1.

Table 1
System specifications.

VZ 4000	
Distance range	1.2 m
Sensor resolution	0.015 mm
Accuracy	0.5 mm RMS
Load cell (DPM-3)	
Read rate	60 Hz
Input voltage	85–264 Vac or 90–300 Vdc
Output voltage	–10 to +10 V
Output current	0–20 mA
Sensor resolution	±0.02% of full-scale analog output
Maximum force	222.41 N (50 lb)
NI myRIO	
# Analog input	10
# Analog output	6
# Digital I/O	40
CPU	Xilinx FPGA & ARM [®] Cortex [™] -A9
Clock rate	40 MHz
Stepper motor (MPK-569-2.8A)	
Phase	5 phase
Step angle	0.72°/step
Voltage	1.75 V
Current	2.8 A/phase
Resistance	0.62 ± 10% Ω/phase
Inductance	1.1 ± 20% mH/phase
Holding torque	16 kgf·cm

2.1 Motion analyses

We invited the therapists to conduct clinical NDT training and observed their actions on the test subjects. The therapists guided the subject's movements using the ropes that were attached to the subject's ASIS. We measured the therapists' applied forces and each subject's motions. The measured data were then analyzed to derive patterns of the therapists' actions.

A complete gait cycle is defined as the period from the initial contact of the stance leg with the ground to the next initial contact of the same leg, as shown in Fig. 2. A gait cycle is conventionally divided into stance and swing phases, with durations of about 60 and 40%, respectively. The stance phase consists of the following periods:⁽²⁴⁾ (1) initial contact, (2) foot flat, (3) mid-stance, (4) heel off, and (5) toe off. The swing phase is composed of (6) initial and mid-swing and (7) terminal swing. The double support periods occur twice, at (1) and (5), during a complete gait cycle and are defined as the duration from when the heel first contacts the ground to when the toes of the other foot take off from the ground.

We tested the trainer and recruited 10 patients to participate in the experiments. The following restrictions were set on the selection of test subjects: (i) the Mini-Mental State Examination (MMSE)⁽²⁵⁾ score should be higher than 24; (ii) the Brunnstrom Stage (BS)⁽²⁶⁾ on the lower extremity is stage 3 to 5; (iii) the Functional Ambulation Category (FAC)⁽²⁷⁾ is stage 3 to 5; (iv) subjects can walk 10 m indoors with or without aid devices; and (v) subjects can stand up with a handrail and aids by themselves. They signed informed consent forms

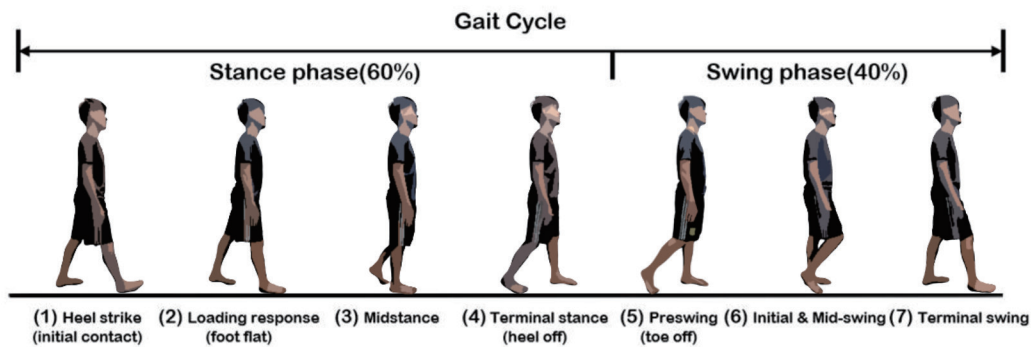


Fig. 2. (Color online) Complete gait cycle.

Table 2
Information of the clinical testing subjects.

Subject	Sex	Age	Height (cm)	Weight (kg)	Paretic side	MMSE (score)	BS (stage)	FAC (stage)
A	Male	56	180	77	Left	30	4	4
B	Male	55	175	82	Right	30	4	4
C	Male	59	182	70	Right	28	4	4
D	Male	71	162	76	Left	30	4	4
E	Male	63	171	70	Left	30	4	3
F	Male	66	168	80	Left	29	4	4
G	Male	65	163	63	Left	30	4	4
H	Male	57	160	58	Right	30	4	4
I	Male	55	155	61	Right	30	4	4
J	Male	55	180	75	Right	30	4	4

approved by the Human Subject Research Ethics Committee of the Institutional Review Board (IRB) (Appendix A). The patients' data are illustrated in Table 2. When the therapist pulled the ropes to guide the subject's gait, we recorded the load-cell data and divided it into gait cycles for analyses (Appendix B). For example, the forces applied on the right ASIS and the height of the left heel of subject C are shown in Fig. 3, where the x -axis represents the percentage of each gait cycle. We can observe that the therapist applied forces on the opposite ASIS approximately when the heel struck the ground, corresponding to periods (1), (4), and (7) of Fig. 2. The actions on other subjects were similar. Therefore, we designed the NDT trainer on the basis of these patterns. Note that the applied forces are small (less than 50 N) and would not harm the users.

The therapists' applied forces on subject C are shown in Figs. 4(a) and 4(b), where the forces were periodic. Taking the fast Fourier transform (FFT) of the force data gives the corresponding frequency responses, as illustrated in Figs. 4(c) and 4(d). In addition, the applied forces on the left and right sides had the same dominant frequency. The analyses for other subjects were similar, as illustrated in Table 3, where different subjects had different dominant frequencies. Because the force profiles are like sinusoidal waves, we can reconstruct them as follows:

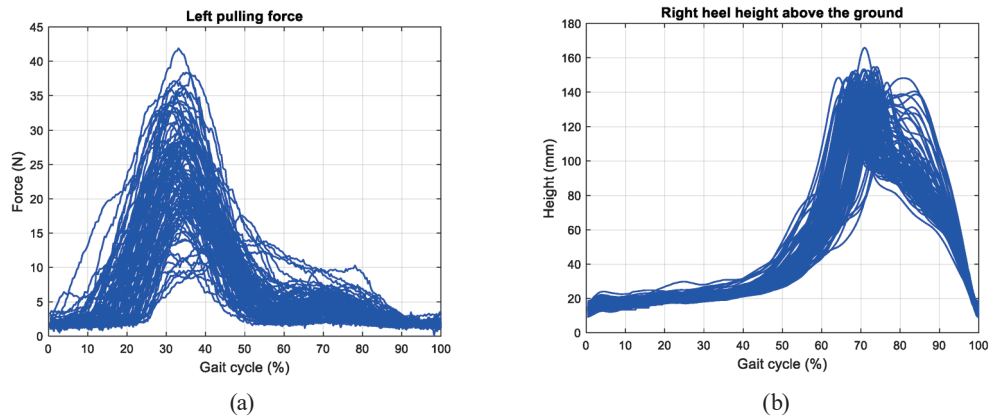


Fig. 3. (Color online) Analyses of the intervention patterns. (a) Forces applied on the right ASIS. (b) Heights of the left heel.

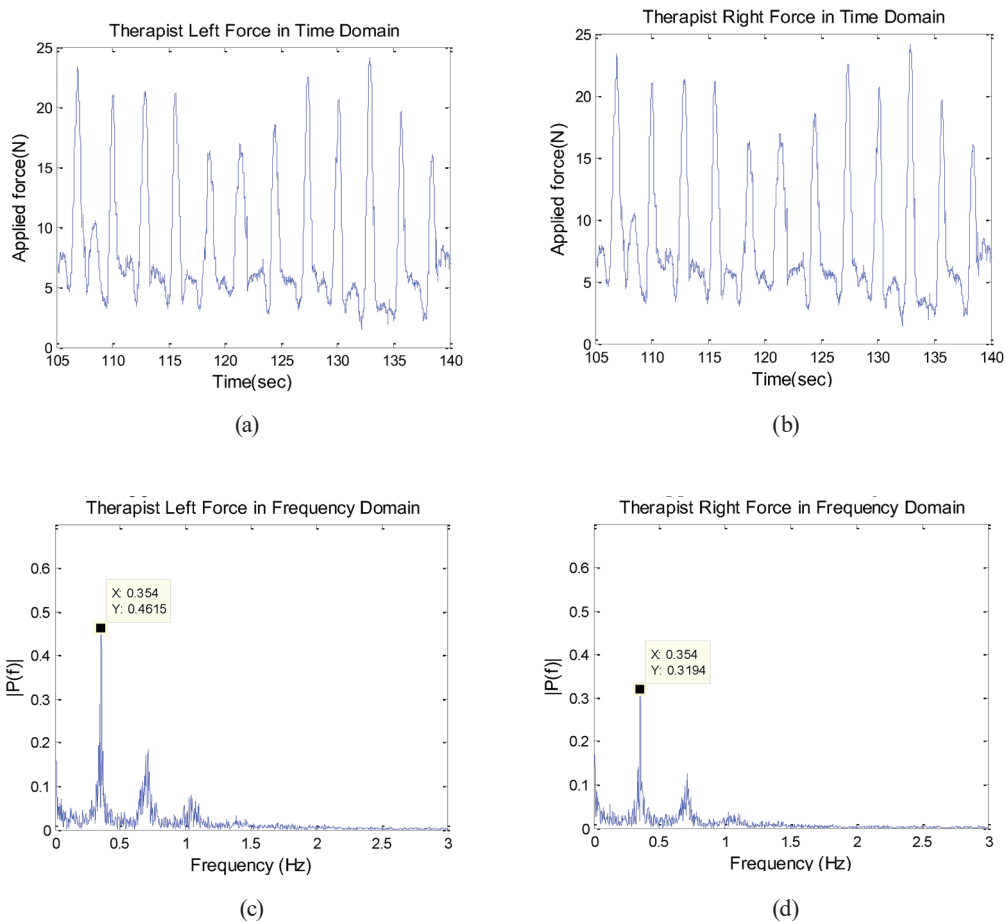


Fig. 4. (Color online) Analyses of the applied forces by the therapist (subject C). (a) Applied force on the left ASIS. (b) Applied force on the right ASIS. (c) FFT of the left applied force. (d) FFT of the right applied force.

Table 3
Parameters of the applied forces on all subjects.

Subject	Paretic side			Non-paretic side		
	F_{max} (N)	F_{min} (N)	f (Hz)	F_{max} (N)	F_{min} (N)	f (Hz)
A	22.5	2.26	0.56	17.5	2.31	0.56
B	26.5	2.26	0.55	20.8	2.31	0.55
C	33.4	2.44	0.35	41.9	2.57	0.35
D	29.1	1.42	0.47	15.4	1.86	0.47
E	34.7	1.24	0.56	26.5	1.20	0.56
F	29.7	1.42	0.51	16.8	1.02	0.51
G	23.5	1.51	0.64	17.6	2.17	0.64
H	19.4	2.44	0.51	20.2	2.00	0.50
I	34.1	2.31	0.91	22.9	1.15	0.91
J	32.2	2.53	0.77	25.6	2.31	0.77

$$(F_{max} - F_{min}) \times \sin(2\pi ft) + F_{min}, \quad (1)$$

where F_{max} and F_{min} represent the average maximum and minimum of the applied forces, respectively, while f is the dominant frequency. Hence, we can build a motor control system to track force commands in the form of Eq. (1). For example, for subject C, the preferred intervention forces are $[(33.4 - 2.44) \times \sin(2\pi ft) + 2.44]$ N on the right ASIS and $[(41.9 - 2.57) \times \sin(2\pi ft) + 2.57]$ N on the left ASIS, where $f = 0.35$ Hz.

2.2 Motor control

The motor control system is shown in Fig. 5, which can repeat the therapists' intervention patterns. We conducted experiments to derive the transfer function of the system and design controllers to track the force commands in the form of Eq. (1). For the identification experiments, the load cells were connected to a stationary rigid body. We then considered the testing subjects as model variations and disturbances, and designed a robust loop-shaping controller to track the force commands during NDT training.

See Appendix C for the identification and controller design of the motor control system. Considering the system variation during operations, we designed a robust controller for the system. First, the nominal plant G_0 was chosen as follows:

$$G_0 = \frac{-21.39s + 339.4}{s^2 + 39.09s + 64.89}, \quad (2)$$

which gave a system gap of 0.0194. The gap can be regarded as the maximum system variation due to system uncertainties and operating conditions. Second, we designed the robust loop-shaping controller by setting the following weighting function:

$$W = \frac{4s + 0.8}{0.1225s^2 + 0.7s + 1}. \quad (3)$$

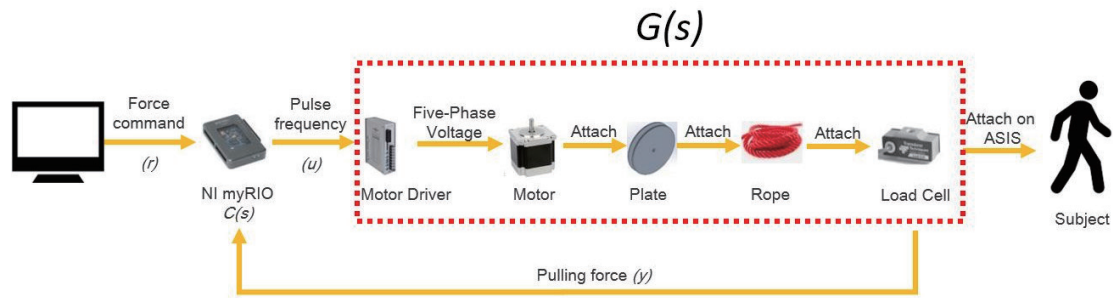


Fig. 5. (Color online) Motor control system.

The robust controller was derived as follows:

$$K_{\infty} = \frac{3.746s^2 + 171.8s + 1131}{s^2 + 84.06s + 5588}, \quad (4)$$

which gave a stability margin of $b(WG_0, K_{\infty}) = 0.2579$. Because the stability margin (0.2579) is much greater than the system gap (0.0194), the system stability can be ensured during operations.

Furthermore, we noted the phase lag of the closed-loop transfer function at the operating frequency, which might result in unsynchronized responses during the training. Therefore, we added a phase-lead pre-compensator, as illustrated in Fig. 6(a), to improve the tracking performance. For example, the phase lag of the closed-loop system at 1 Hz is about 35° . Therefore, the phase-lead pre-compensator was designed as

$$C_{pre}(s) = 0.737 \frac{s/6.5 + 1}{s/40 + 1}, \quad (5)$$

which gave a phase lead of about 35° at 1 Hz. Before the clinical tests, we connected the rope to a stationary rigid body to test the motor's tracking ability to the following force command:

$$r = [(26.68 - 6.67) \times \sin(2\pi t) + 6.67] \text{ N}. \quad (6)$$

The simulation and experiment results are shown in Fig. 6(b), where the phase lag was successfully eliminated by the phase-lead pre-compensator. In addition, the root mean square errors of the simulation and experiments are 0.21 and 2.14 N, respectively. The experimental tracking errors are much higher than the simulation errors, because unmodeled dynamics and disturbances might be introduced during the experiments. Nevertheless, the designed motor control mechanism can track the desired force patterns. We tried to apply simple control, such as proportional-integral-derivative control, to the motor system. However, the responses were

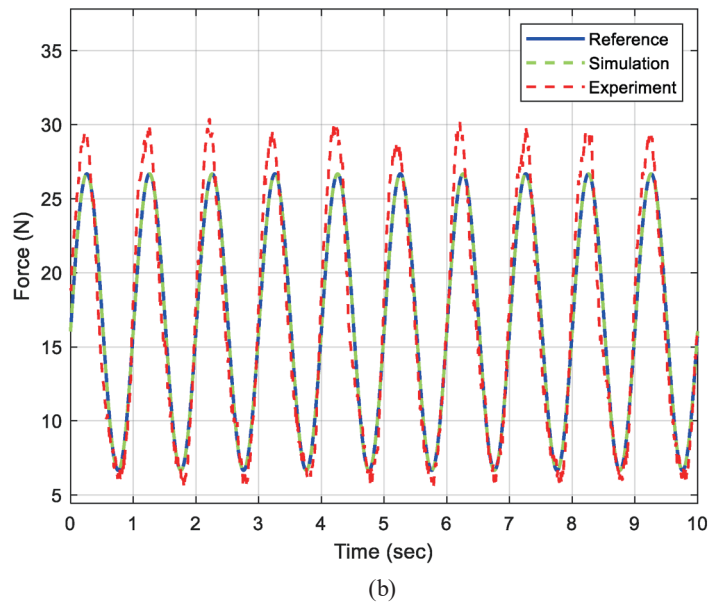
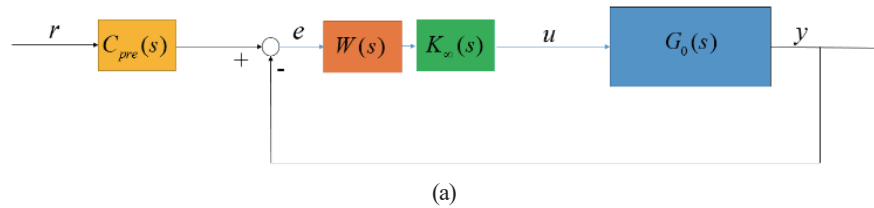


Fig. 6. (Color online) Control design and force responses of the motor control system. (a) Motor control system with the pre-compensator. (b) Force-tracking responses.

much worse than those using the robust control because of unmodeled dynamics and system disturbances during experiments. Hence, we implemented the designed robust control in the motor system.

2.3 Control procedures

We observed that the therapist applied forces on the opposite ASIS approximately when the heel struck the ground during the clinical NDT rehabilitation, as shown in Fig. 3. Therefore, we applied this principle to the motor control system to imitate the therapist's actions, where the motors should be controlled according to the opposite heel strikes. For example, the left motor begins to pull the rope according to Eq. (1) when the right heel strikes the ground and is in front of the left heel, as illustrated in Fig. 7(a). The pulling force is then kept at the minimum value as the cycle is completed or when the right heel leaves the ground. The right motor is operated in a similar way. Because the VZ 4000 motion capture system has a high resolution of 0.015 mm, the developed algorithm illustrated in Fig. 7(a) can detect the heel strikes with a success rate of 95–99%. If the system fails to detect a heel strike, the motors will follow a constant force

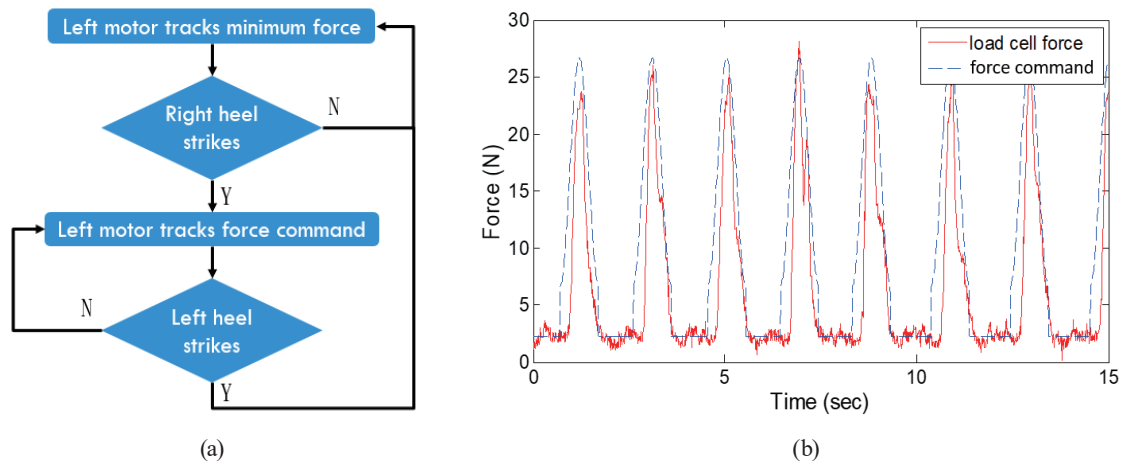


Fig. 7. (Color online) Automated NDT control algorithm and force tracking responses. (a) Flow chart of motor control. (b) Force tracking during NDTs.

command of $F_{min} = 1\text{--}3$ N (see Table 3), which will not harm users. We connected the rope to the test subject's ASIS and set $F_{max} = 26.68$ N, $F_{min} = 2.22$ N, $f = 1$ Hz. The experimental results are shown in Fig. 7(b), where the motor can track the force commands during NDT training. In contrast to the responses in Fig. 6(b), those in Fig. 7(b) showed that human dynamics were introduced when the trainer was applied to the subjects. However, the designed robust controller can effectively cope with these unmodeled dynamics and disturbances when conducting NDT training.

3. Results and Discussion

We recruited 10 stroke patients (see Table 2) to undergo NDT training. All subjects signed informed consent forms approved by the Human Subject Research Ethics Committee of the IRB before participating. We recorded the gait data using the VZ 4000 and defined a performance index to evaluate the effectiveness of rehabilitation.

Because gait asymmetry is a critical pattern for post-stroke walking rehabilitation, guiding the paralyzed side to shift the COG at the right time is the key point for initiating the stepping. In addition, reciprocal and repeated training can help patients to accumulate experience from comparison with the sound side. Therefore, we define the following performance index to assess the effectiveness of rehabilitation:⁽²⁸⁾

$$\text{Asymmetry of the swing phases: } Asym_{SP}(\%) = \frac{SP_{paretic} - SP_{non-paretic}}{SP_{paretic}} \times 100\%, \quad (7)$$

where $SP_{paretic}$ and $SP_{non-paretic}$ represent the swing phases of the paretic and non-paretic limbs, respectively. The swing phase of a leg is defined as the duration from the toe off to the

heel strike of the leg. For example, $SP_{paretic}$ and $SP_{non-paretic}$ represent the swing phases of the left and right limbs, respectively; for patients with left-side paresis, NDT is expected to reduce the deviation in the swing phases of the two sides.⁽²⁸⁾ Therefore, the treatment is considered effective when the asymmetry approaches zero. We compared the effects of the NDT training by therapists and by the proposed trainer.

Ten subjects participated in the tests. We recorded and analyzed their gait data by the following $A - B - \bar{A}$ procedures: before treatment (A), in treatment (B), and after treatment (\bar{A}), to observe the effectiveness of the NDT. We set the interval of B to about twice the intervals of A and \bar{A} to enhance the training effect. Eight test subjects (A, B, C, D, E, H, I, and J) were first guided by the therapists through the $A_{th} - B_{th} - \bar{A}_{th}$ procedure, where the subscript th indicates the training conducted by therapists. The subjects then rested for about 30 mins before being guided by the proposed NDT trainer through the $A_{mot} - B_{mot} - \bar{A}_{mot}$ procedure, where the subscript mot indicates the training conducted by the motor control system. Two test subjects (F and G) were guided by the automatic trainer first, then by therapists. Note that the training order was randomly assigned. One trial was conducted on each subject. The asymmetry of the swing phases $Asym_{SP}$ calculated from the experimental responses is illustrated in Fig. 8, where the number of gait cycles varied because each subject had a different walking speed and the therapists might have adjusted the training time according to the subjects' conditions.

From Fig. 8, the improvement by NDT guiding is notable during the in-treatment (B) and after-treatment (\bar{A}) periods. For quantitative comparison, we further calculated the average

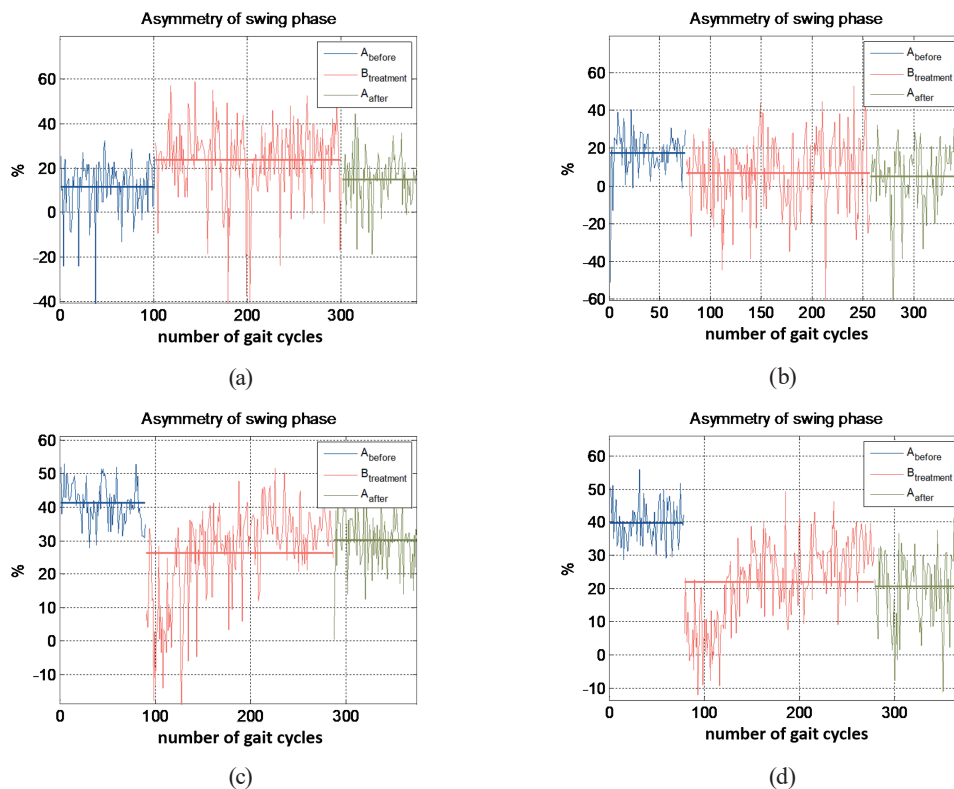


Fig. 8. (Color online) Experimental responses of the asymmetry of the swing phases. (a) Subject A: therapist guiding. (b) Subject A: motor guiding. (c) Subject B: therapist guiding. (d) Subject B: motor guiding.

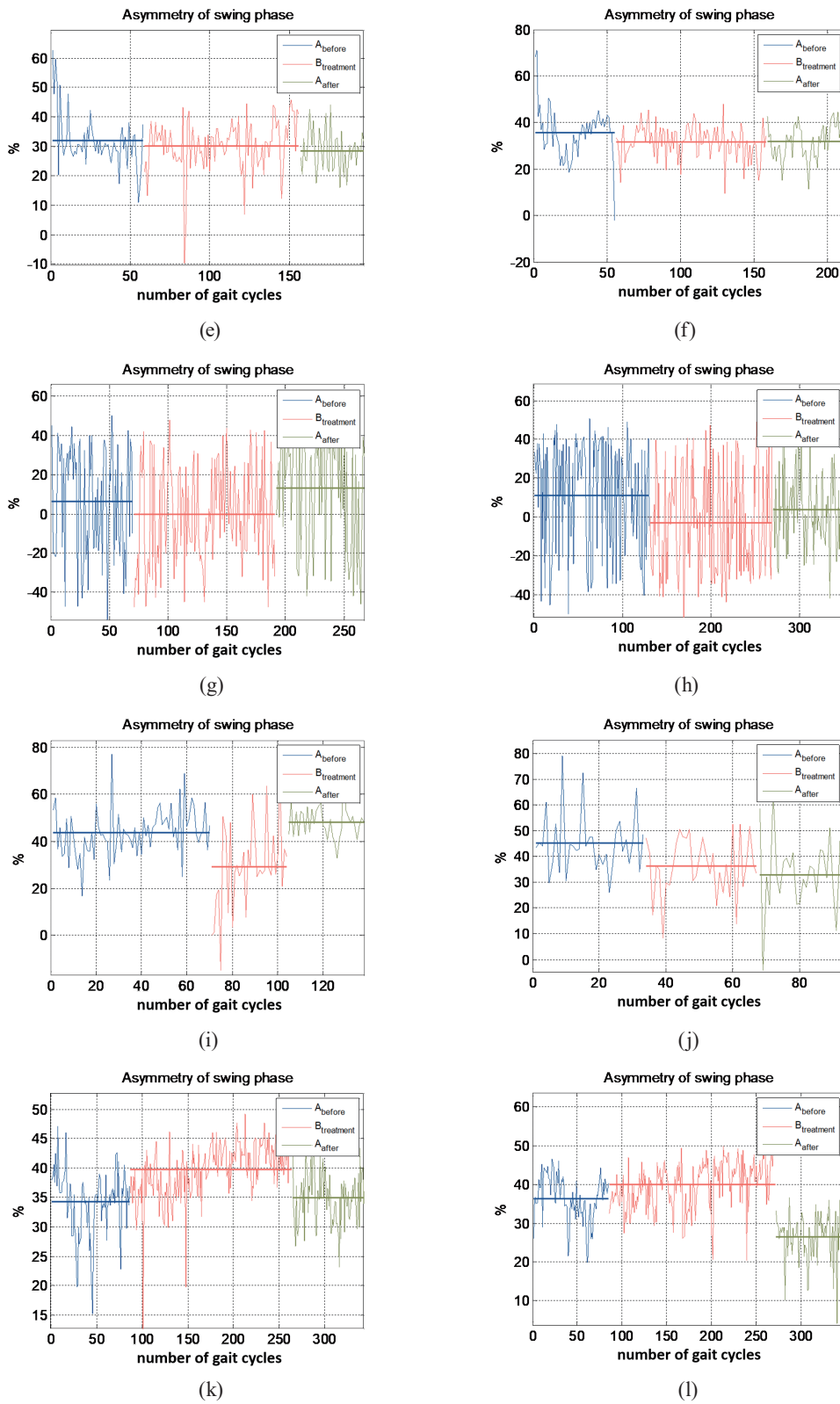


Fig. 8. (Color online) (continued) Experimental responses of the asymmetry of the swing phases. (e) Subject C: therapist guiding. (f) Subject C: motor guiding. (g) Subject D: therapist guiding. (h) Subject D: motor guiding. (i) Subject E: therapist guiding. (j) Subject E: motor guiding. (k) Subject F: therapist guiding. (l) Subject F: motor guiding.

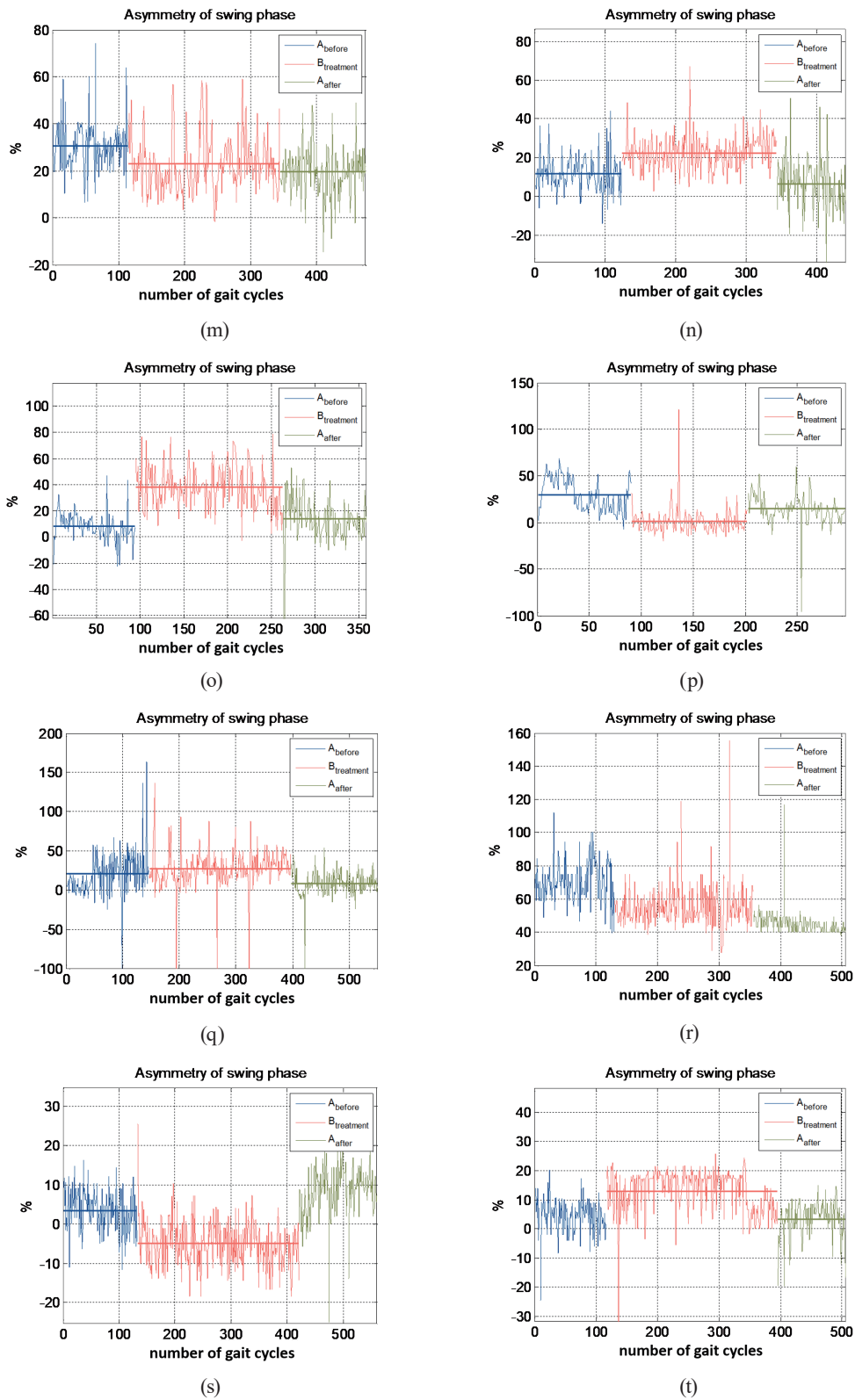


Fig. 8. (Color online) (continued) Experimental responses of the asymmetry of the swing phases. (m) Subject G: therapist guiding. (n) Subject G: motor guiding. (o) Subject H: therapist guiding. (p) Subject H: motor guiding. (q) Subject I: therapist guiding. (r) Subject I: motor guiding. (s) Subject J: therapist guiding. (t) Subject J: motor guiding.

Table 4
Asymmetry of the swing phases $Asym_{SP}$ (%) from Fig. 8.

Subject	Therapist guiding			NDT trainer guiding		
	A_{th}	B_{th}	\bar{A}_{th}	A_{mot}	B_{mot}	\bar{A}_{mot}
Patient A	11	24	15	17	7	5
Patient B	41	26	30	40	22	21
Patient C	32	30	28	36	32	32
Patient D	6	0	13	11	-2	3
Patient E	43	29	48	45	39	32
Patient F	36	39	26	34	39	34
Patient G	11	22	6	30	22	19
Patient H	8	38	14	30	4	14
Patient I	20	28	9	74	56	43
Patient J	3	-5	9	5	-2	3

($_{th}$: therapist guiding; $_{mot}$: trainer guiding)

asymmetry of the swing phases $Asym_{SP}$ in each procedure, as illustrated in Table 4. A_{th} , B_{th} , and \bar{A}_{th} represent before treatment, in treatment, and after treatment, respectively, by the therapists. A_{mot} , B_{mot} , and \bar{A}_{mot} represent before treatment, in treatment, and after treatment, respectively, by the motor-controlled trainer. The values are in bold if they are improved.

Reestablishment of gait asymmetry in stroke patients is an important goal of rehabilitation. The patients with a stroke on the right hemiparesis usually have a longer swing time on the right side than on the left side, and vice versa. As indicated in Table 4, the asymmetry of the swing phases was generally improved during the treatment (B_{mot}) and after treatment (\bar{A}_{mot}) by the proposed NDT trainer. In addition, the asymmetry after treatment (\bar{A}_{th} and \bar{A}_{mot}) was generally improved; i.e., the rehabilitation efficacy was sustained even after the treatment. In addition, the improvements by the NDT trainer guidance (B_{mot} and \bar{A}_{mot}) were more significant than those by the therapist guidance (B_{th} and \bar{A}_{th}). One possible reason was that the trainer provided objective judgments and did not become fatigued. Furthermore, patients F and G were guided by the automatic trainer first, so that their improvement after treatment by the therapists (\bar{A}_{th}) was both greatly improved. That is, the subjects gradually became familiar with the intervention by repeating exercises through the trainer.

The test results revealed positive training effects for short-term intervention. That is, the proposed automated NDT trainer can repeat the therapist's actions on the test subjects, so it can relieve the therapist's workload and increase the patient's training time. In addition, the effectiveness of the treatment can be sustained after the training. Because the NDT program is a long-term training process and the effectiveness of training might be gradually improved, we plan to carry out long-term training tests in the future to evaluate the improvement.

4. Conclusions

We have developed an automated NDT trainer. NDT rehabilitation is effective because it provides guided and induced interventions to achieve motor learning effects. However, traditional NDT rehabilitation is labor-intensive for therapists, meaning that patients usually

receive insufficient training due to the shortage of therapist assistance. Therefore, we analyzed the clinical key points during NDT training and constructed a motor mechanism to imitate the therapists' intervention. First, we recruited therapists and patients to conduct clinical NDTs. During the clinical NDT rehabilitation, we applied a motion capture system (VZ 4000) and load cells (DPM-3) to record the test subjects' motions and the therapists' applied forces, respectively. Then, we analyzed the recorded data to build an expert system that described the intervention patterns. Second, we applied this expert system to construct a motor control mechanism that can detect the user's motions by the VZ 4000 and repeat the therapist's actions using a closed-loop motor control system. Third, we integrated the system and conducted experiments on 10 test subjects. Their gaits were measured to evaluate the effectiveness of rehabilitation following guidance by therapists and by the designed NDT trainer. The results confirmed that the proposed NDT trainer significantly improved the rehabilitation effects in terms of gait asymmetry. Furthermore, the performance improvement by the trainer guidance was occasionally even better than the improvement by the therapist guidance. One possible reason is that the trainer provided objective judgments and did not become fatigued. As a prototype, the proposed trainer can provide NDT rehabilitation effects on stroke patients, while reducing therapists' workloads and increasing patients' training time.

In the future, we plan to recruit more subjects to conduct long-term training to verify the effectiveness of the automated NDT trainer. In addition, we wish to explore more decision parameters of therapists, such as the balance of COG and lateral symmetry,^(29,30) to further understand therapists' intervention decisions and training methods for stroke rehabilitation.

Acknowledgments

The authors would like to thank Mr. Tien-Yun Kuo for helping with the manuscript preparation. This work was financially supported in part by the Joint Project between Industrial Technology Research Institute of Taiwan and National Taiwan University under Grants 104-MSL01 and 105-MSL01. This research was also financially supported in part by the Ministry of Science and Technology of Taiwan under Grants MOST 107-2221-E-002-174, MOST 107-2634-F-002-018 -, MOST 108-2634-F-002-016 -, and MOST 109-2634-F-002-027 - and National Taiwan University, Center for Artificial Intelligence & Advanced Robotics.

References

- 1 Ministry of Health and Welfare of ROC: Department of Statistics. Ten Leading Causes of Death, <https://www.mohw.gov.tw/cp-3425-33347-2.html> (accessed July 2020).
- 2 M. J. Hall, S. Levant, and C. J. DeFrances: NCHS Data Brief. **95** (2012) 1. <https://www.ncbi.nlm.nih.gov/pubmed/22617404>
- 3 A. S. Go, D. Mozaffarian, V. L. Roger, E. J. Benjamin, J. D. Berry, M. J. Blaha, S. Dai, E. S. Ford, C. S. Fox, S. Franco, H. J. Fullerton, C. Gillespie, S. M. Hailpern, J. A. Heit, V. J. Howard, M. D. Huffman, S. E. Judd, B. M. Kissela, S. J. Kittner, D. T. Lackland, J. H. Lichtman, L. D. Lisabeth, R. H. Mackey, D. J. Magid, G. M. Marcus, A. Marelli, D. B. Matchar, D. K. McGuire, E. R. MohlerIII, C. S. Moy, M. E. Mussolino, R. W. Neumar, G. Nichol, D. K. Pandey, N. P. Paynter, M. J. Reeves, P. D. Sorlie, J. Stein, A. Towfighi, T. N. Turan, S. S. Virani, N. D. Wong, D. Woo, and M. B. Turner: *Circulation* **129** (2014) 8. <https://doi.org/10.1161/01.cir.0000442015.53336.12>

- 4 I. Díaz, J. J. Gil, and E. Sánchez: *J. Robot.* **2011** (2011) 1. <https://doi.org/10.1155/2011/759764>
- 5 G. Colombo, M. Joerg, R. Schreier, and V. Dietz: *J. Rehab. Res. Dev.* **37** (2000) 6. <https://www.ncbi.nlm.nih.gov/pubmed/11321005>
- 6 D. J. Reinkensmeyer, D. Aoyagi, J. L. Emken, J. A. Galvez, W. Ichinose, G. Kerdanyan, S. Maneeakobkunwong, K. Minakata, J. A. Nessler, R. Weber, R. R. Roy, R. de Leon, J. E. Bobrow, S. J. Harkema, and V. R. Edgerton: *J. Rehab. Res. Dev.* **43** (2006) 657. <https://doi.org/10.1682/JRRD.2005.04.0073>
- 7 H. Schmidt, C. Werner, R. Bernhardt, S. Hesse, and J. Kruger: *J. NeuroEng. Rehab.* **4** (2007). <https://doi.org/10.1186/1743-0003-4-2>
- 8 F. C. Wang, C. H. Yu, and T. Y. Chou: *Proc. Inst. Mech. Eng. H: J. Eng. Med.* **223** (2009) 687. <https://doi.org/10.1243/09544119JEIM609>
- 9 J. Patton, D. A. Brown, M. Peshkin, J. J. Santos-Munné, A. Makhlin, and E. Lewis: *KineAssis: Top. Stroke Rehab.* **15** (2008) 131. <https://doi.org/10.1310/tsr1502-131>
- 10 A. Esquenazi, M. Talaty, A. Packel, and M. Saulino: *Am. J. Phys. Med. Rehab.* **91** (2012) 911. <https://doi.org/10.1097/PHM.0b013e318269d9a3>
- 11 C. Schmitt and P. Métrailler: *Proc. 8th Vienna Int. Workshop Functional Electrical Stimulation.* **11** (2004) 117–120. <https://infoscience.epfl.ch/record/81393>
- 12 D. Bradley, C. Acosta-Marquez, M. Hawley, S. Brownsell, P. Enderby, and S. Mawson: *Mechatronics* **19** (2009) 247. <https://doi.org/10.1016/j.mechatronics.2008.07.006>
- 13 G. Belforte, L. Gastaldi, and M. Sorli: *Mechatronics* **11** (2001) 301. [https://doi.org/10.1016/S0957-4158\(00\)00017-9](https://doi.org/10.1016/S0957-4158(00)00017-9)
- 14 H. Yu, S. Huang, G. Chen, and N. Thakor: *Mechatronics* **23** (2013) 1072. <https://doi.org/10.1016/j.mechatronics.2013.08.004>
- 15 M. Pohl, J. Mehrholz, C. Ritschel, and S. Rückriem: *Stroke* **33** (2002) 553. <https://doi.org/10.1161/hs0202.102365>
- 16 J. S. Vj and N. K. Multani: *Physiotherapy* **8** (2012) 30. <https://doi.org/10.1016/j.physio.2015.03.1599>
- 17 E. Mikołajewska: *Adv. Clin. Exp. Med.* **22** (2013) 261. <https://www.ncbi.nlm.nih.gov/pubmed/23709383>
- 18 M. Visintin, H. Barbeau, N. Korner-Bitensky, and N. E. Mayo: *Stroke* **29** (1998) 1122. <https://doi.org/10.1161/01.STR.29.6.1122>
- 19 S. Hesse, C. Bertelt, M. T. Jahnke, A. Schaffrin, P. Baake, M. Malezic, and K. H. Mauritz: *Stroke* **26** (1995) 976. <https://doi.org/10.1161/01.STR.26.6.976>
- 20 Phoenix Technologies Inc. VZ 4000 tracker: <https://www.ptiphoenix.com/?prod-trackers-post=vz4000> (accessed July 2020).
- 21 Transducer Techniques. DPM-3: <https://www.transducertechniques.com/load-cell-displays.aspx> (accessed July 2020).
- 22 T. D. Collins, S. N. Ghoussayni, D. J. Ewins, and J. A. Kent: *Gait Posture* **30** (2009) 173. <https://doi.org/10.1016/j.gaitpost.2009.04.004>
- 23 National Instrument. NI myRIO-1900: <https://sine.ni.com/nips/cds/view/p/lang/zht/nid/211694> (accessed July 2020).
- 24 EpoMedicine. Normal Gait Cycle: <https://epomedicine.com/clinical-medicine/physical-examination-gait/> (accessed July 2020).
- 25 D. Mungas: *Geriatrics* **46** (1991) 54. <https://www.ncbi.nlm.nih.gov/pubmed/2060803>
- 26 Saebo: The Brunnstrom Stages of Stroke Recovery, <https://www.saebo.com/the-stages-of-stroke-recovery/> (accessed July 2020).
- 27 M. K. Holden, K. M. Gill, and M. R. Magliozzi: *Phys. Ther.* **66** (1986) 1530. <https://doi.org/10.1093/ptj/66.10.1530>
- 28 G. Chen, C. Patten, D. H. Kothari, and F. E. Zajac: *Gait Posture* **22** (2005) 51. <https://doi.org/10.1016/j.gaitpost.2004.06.009>
- 29 K. J. Dodd and M. E. Morris: *Arch. Phys. Med. Rehab.* **84** (2003) 1200. [https://doi.org/10.1016/S0003-9993\(03\)00142-4](https://doi.org/10.1016/S0003-9993(03)00142-4)
- 30 K. J. Dodd, M. E. Morris, T. A. Matyas, T. V. Wrigley, and P. A. Goldie: *Gait Posture* **7** (1998) 243. [https://doi.org/10.1016/S0966-6362\(98\)00013-7](https://doi.org/10.1016/S0966-6362(98)00013-7)
- 31 National Taiwan University Hospital, Clinical Trial Center: <https://www.ntuh.gov.tw/NCTRC/training/training.aspx> (accessed July 2020).

Appendix A: Ethical Review Approval

The informed consent forms approved by the Human Subject Research Ethics Committee of the IRB are available (http://140.112.14.7/~sic/PaperMaterial/Sensors_and_Materials_A.pdf).⁽³¹⁾

Appendix B: Therapists' Intervention on Patients

The intervention pattern data of the 10 test subjects are available (http://140.112.14.7/~sic/PaperMaterial/Sensors_and_Materials_B.pdf).

Appendix C: System Identification and Robust Control Design

The system identification and robust control design are available (http://140.112.14.7/~sic/PaperMaterial/Sensors_and_Materials_C.pdf).

About the Authors



Fu-Cheng Wang received his B.S. and M.Sc. degrees from the Mechanical Engineering Department, National Taiwan University, and his Ph.D. degree in control engineering from the Engineering Department, Cambridge University, U.K. He joined the Mechanical Engineering Department of National Taiwan University in 2003. His research interests include robust control, vibration control, system integration, medical engineering, fuel cell control, energy systems, and embedded systems. (fcw@ntu.edu.tw)



Yu-You Lin received his B.S. degree from the Department of Mechanical Engineering, National Central University, in 2015 and his M.Sc. degree from the Mechanical Engineering Department, National Taiwan University, in 2017. His current research interests include robust control, system integration, biomedical engineering, and embedded systems. (r04522815@ntu.edu.tw)



You-Chi Li received his B.S. degree from the Department of Mechanical Engineering, National Central University, in 2017. He is currently studying toward his M.S. degree at the Mechanical Engineering Department, National Taiwan University. His current research interests include robust control, system integration, biomedical engineering, and AI models. (p284fu6@gmail.com)



Po-Yin Chen received his B.S., M.Sc., and Ph.D. degrees from the Department of Physical Therapy and Assistive Technology, National Yang-Ming University, and is a physical therapist in Taiwan. His specialties are balance and gait training in physical therapy and rehabilitation engineering. (azxd32@hotmail.com)



Chung-Huang Yu received his B.S. and M.Sc. degrees in mechanical engineering from National Taiwan University, Taipei, Taiwan, and his Ph.D. degree in medical physics and bioengineering from University College London, U.K. He is an associate professor in the Department of Physical Therapy and Assistive Technology, National Yang-Ming University. His research interests include intelligent assistive system design, rehabilitation engineering, mechatronic systems, and biomechanics. (chyu@ym.edu.tw)